

PROTON SCATTERING FROM A TUNGSTEN SINGLE CRYSTAL

A. F. TULINOV, V. S. KULIKAUSKAS and M. M. MALOV
Institute of Nuclear Physics, Moscow University, Moscow, USSR

Received 26 July 1965

Usually amorphous or polycrystalline targets are used for studying nuclear reactions initiated by accelerated particles. It has been shown [1,2] that if a single crystal target is used, dips in the direction of the crystalline axes appear in the angular distribution of charged reaction products. The intensity decrease in the dip was attributed to the Coulomb scattering of the reaction products by the relevant nuclear chain. This effect was found experimentally in studying the elastic scattering of protons from a tungsten single crystal. The present paper contains a study on the influence of different factors on the effect in question.

The measurements were carried out using the 120 cm cyclotron of the Institute of Nuclear Physics at Moscow University. The proton energy was changed with absorbers; a 2 mm thick tungsten single crystal was used as a target. The crystalline axis corresponding to the shortest distance between lattice sites was used. Since tungsten has a body centered cubic lattice the axis [111] meets this condition ($l = 2.7 \text{ \AA}$). The direction of the axis was determined with an X-ray method. The sample was fastened to a copper rod connected to a cryostat. The beam diameter was 1 mm. The angle between the crystal surface and the direction of the beam was 30° , with the [111]

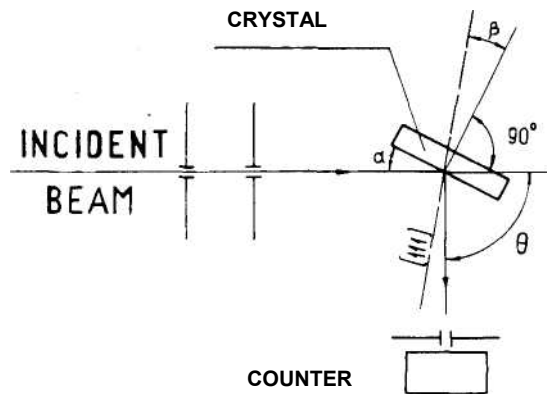
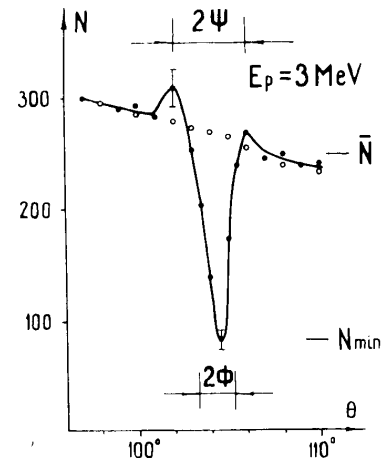


Fig. 1. General sketch of the experiment.

measured near the direction of the $[111]$ axis axis in the horizontal plane, forming an angle $\beta = 15^\circ$ to the normal on the surface (fig. 1). The angular distribution of elastically scattered protons was. The protons were detected by a system of two junction detectors, each of them 4 mm in diameter. The counters were at a distance of 45 cm from the target. One of them could be rotated in the horizontal plane and the other in the vertical plane, without breaking the vacuum. A third junction detector placed at a fixed angle with respect to the direction of the beam was used as a monitor. Pulses from the detectors were led to a 100-channel amplitude analyser. For control measurements the sample could be replaced by a polycrystalline target without disturbing the vacuum. Shown in fig. 2 is the proton angular distribution corresponding to a beam energy of $E_p = 3$ MeV. Plotted as the ordinate are the numbers of pulses corresponding to the high energy part of the continuous spectrum (the threshold was at 80% of the maximum signal). The circles denote the results obtained when a polycrystalline target was used. To make sure that the dip thus obtained was associated with the crystalline axis, the target was rotated in the horizontal plane, which made the dip shift accordingly.

The measurements described above were carried out at room temperature ($T \sim 300^\circ\text{K}$). The heating of the target under the influence of the beam was insignificant. In order to study the temperature dependence of the effect, the crystal was cooled down to liquid nitrogen temperature ($T \sim 80^\circ\text{K}$). The angular distribution for this case is shown in fig. 3. It is seen that, as the temperature falls, both the depth and the width of the dip increase.

Fig. 2. Angular distribution of protons elastically scattered from a tungsten single crystal near the $[111]$ axis at $E_p = 3$ MeV.

o - polycrystalline target.
• - single crystal target.

A change in the proton energy causes a change in the width of the dip without any significant change in its general form. Thus, at $E_p = 6$ MeV,

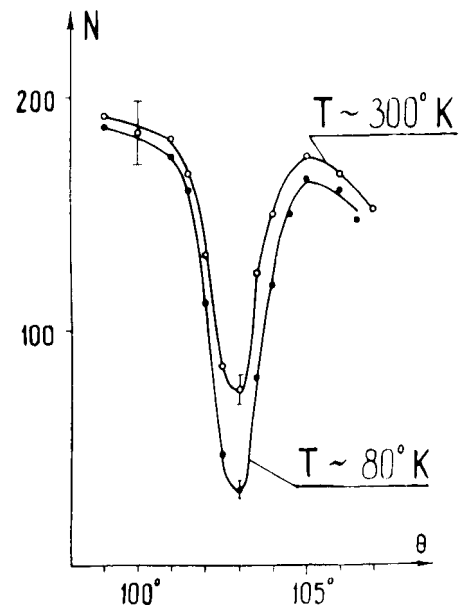


Fig. 3. Temperature dependence of the angular distribution of protons elastically scattered from a tungsten single crystal.

the half-width of the hole was about 1.2° and the distance between the side maxima was about 3° . Since a thick target was used for the measurements, it was of interest to examine the influence of the depth of the layer where the scattering was taking place. To this end, pulse spectra were taken at different angles. These spectra were divided into regions of 10 channels each. Evidently, every region can be associated with a certain depth of the crystal layer causing the scattering. Shown in fig. 4 is the dependence of the depth of the dip on pulse size. The lower curve is for room temperature, the upper one for liquid nitrogen temperature. Apparently, the dip gets broader and shallower with increasing depth of the scattering layer.

In order to estimate the width of the dip the angles ψ and ϕ were used in refs. 1 and 2. The first of these values, ψ , is the minimum scattering angle of a charged particle, when the nuclei of the scattering chain are fixed at the lattice sites. This value may be shown to determine the exterior dimensions of the hole; it is close to the distance between the side maxima. Let the interaction potential of the reaction product (charge Z_1e) and the scattering nucleus (charge Z_2e) be

$$V = \frac{Z_1 Z_2 e^2}{r} e^{-r/a}$$

Then it can be shown that

$$\psi^2 = 2 \frac{b}{l} \left[K_0 \left(\frac{\sqrt{bl}}{a} \right) + 2 \right]$$

where $b = Z_1 Z_2 e^2/a$, l is the distance between the nuclei of the scattering chain, E is the energy of the particle, K_0 is the modified Hankel

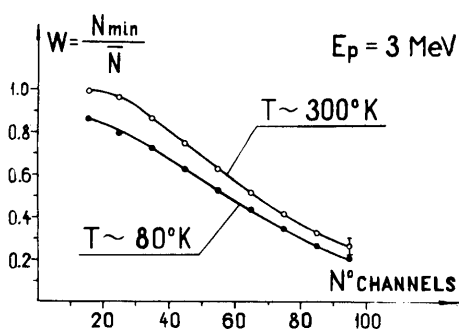


Fig. 4. Relative minimum counting rate in the dip as a function of pulse size, at two different target temperatures.

function. Assuming that $a = 0.5/Z^{1/3}$ A and $E_p = 3$ MeV we obtain $2\psi = 3.3^\circ$. From fig. 2 one obtains $2\psi_{\text{exp}} \sim 4^\circ$.

The second value ϕ is the average scattering angle. It applies to particles emitted by nuclei on the chain axis, with the nuclei of the chain forming a system of independent three-dimensional classical oscillators. This value gives some idea of the average width of the dip. It may be calculated from the following relation

$$\phi^2 = \left[\frac{3}{2} \frac{b^2}{gl} \ln \frac{a}{b} \right]^{2/3} + 2 \frac{b}{l} K_0 \left(\frac{g}{a} \right)$$

where g is the amplitude of nuclear vibrations, which may be estimated using a Debye model of the tungsten lattice. At room temperature $g \approx 1.2 \times 10^{-9}$ cm. Hence $2\phi = 2^\circ$ which is in qualitative agreement with fig. 2. At $T \sim 80^\circ\text{K}$, $g \sim 0.7 \times 10^{-9}$ cm hence $2\phi_{\text{theor}} = 2.6^\circ$ which is also in qualitative agreement with the data of fig. 3. The above relation may also be used to see how the width of the dip depends on the proton energy E_p . At $E_p = 6$ MeV, one obtains $2\psi = 2.5^\circ$ and which values are consistent with the data given above.

The fact that the width of the dip increases with the depth of the scattering layer may be understood as follows. Protons emerging from the internal part of the sample pass through a thick layer and suffer multiple scattering.

How the depth of the dip depends on the position of the reflecting layer is not quite clear yet. It is possible that the effect of particle channeling shows up here [3]. If this is the case, the particles may be accumulated in the channels. This seems to be consistent with fig. 4. These problems are under study at present.

It would also be of interest to investigate the α -decay of nuclei inserted into the lattice of a single crystal. The corresponding anisotropy has been described recently [4].

The authors are indebted to a number of workers of the Department of Physics of Moscow State University, especially to N. B. Brandt, V. K. Zubenko, G. A. Iferov, E. V. Kolontsova and V. E. Urasova.

Addendum

Recently, some experiments were carried out using nuclear emulsion for the detection of scattered protons. The plane of the emulsion was perpendicular to the [100] axis of a tungsten single crystal. The intensity pattern obtained at $E_p = 200$ keV is shown in fig. 5. The dots and lines correspond to the intersections of the

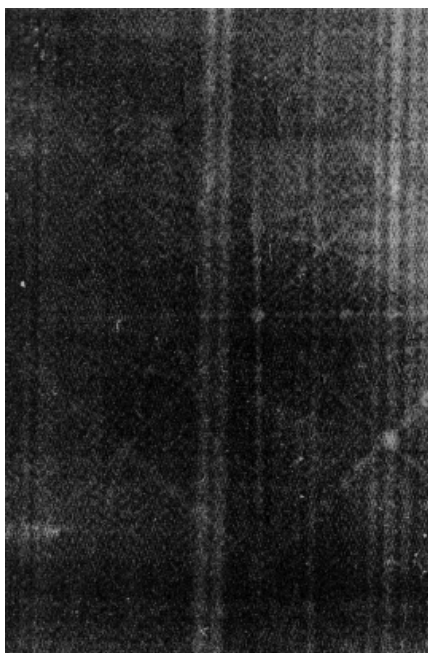


Fig. 5. Angular distribution of protons elastically scattered from a tungsten single crystal at $E_p = 200$ keV. The photoplate was placed perpendicular to the $[100]$ axis.

crystallographic axes and planes, respectively, with the plane of the emulsion. Some of the axes are indicated schematically in fig. 6. The details of the experimental method will be published elsewhere [5].

Apparently, this photographic method is a straightforward and promising way of investigating complex crystal structures.

1. A.F.Tulinov, Report at the XV Annual Nuclear Spectroscopy and Nuclear Structure Conference, January, 1965, Minsk (USSR).

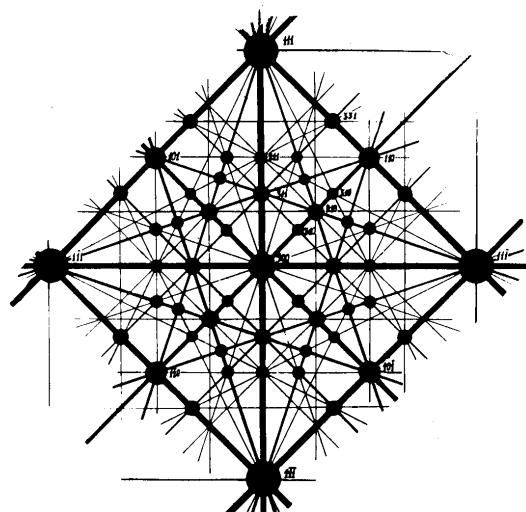


Fig. 6. The solid lines are the intersections of the crystallographic planes with the plane which is perpendicular to the $[100]$ axis. The numbers are indices of the crystallographic axes.

2. A.F.Tulinov, Dokl.Akad.Nauk USSR 162 (1965) 546.
3. I.Lindhard, Physics Letters 12 (1964) 126;
E.Bogh, I.A.Davies and K.O.Nielsen, Physics Letters 12 (1964) 129;
M.W.Thompson, Phys. Rev. Letters 13 (1964) 756.
4. B.Domeij and K.Bjorkqvist, Physics Letters 14 (1964) 127.
5. A.F.Tulinov, B.G.Akhmetova, A.A.Pusanov and A. A.Bednjakov, submitted to Zh.Eksperim. i Teor. Fiz. (USSR).